18th Brazilian Congress of Thermal Sciences and Engineering
November 16-20, 2020 (Online)

ENC-2020-0251
NUMERICAL ANALYSIS OF THE NATURAL CONVECTIVE HEAT TRANSFER FROM HORIZONTAL SURFACES CONTAINING TRAPEZOIDAL WAVES WITH VARIABLE HEIGHT

Nickolas Castro Bernardini
Santiago del Rio Oliveira
Department of Mechanical Engineering, São Paulo State University, 14-01 Engenheiro Luiz Edmundo Carrijo Coube Avenue, Bauru, SP, 17033-360, Brazil.
nickolas.bernardini@gmail.com, santiago.oliveira@unesp.br

Abstract. *This article consists of a numerical analysis of the natural convective heat transfer from horizontal surfaces containing a wavy surface on one side. The wavy surface considered in this project have a trapezoidal shape with variable height, having the effect of increasing the heat transfer rate from the heated surface to an adjacent fluid, in this case, ambient air. The main objective of this work was to calculate the natural convective heat transfer rate between the wavy horizontal surface and the ambient air. Effects on the natural convective heat transfer rate from the surface containing trapezoidal waves were analyzed as a function of the following variables: number of waves, profile of wavy heights, ratio between the largest base and smallest base of the waves and the Rayleigh number. Results were obtained numerically using the standard* $k-\varepsilon$ *turbulence model including effects of buoyant forces with the aid of the commercial CFD solver ANSYS FLUENT©. Recommendations were made according to the profiles of wavy heights that provided the greatest improvement in natural convective heat transfer rate from the heated horizontal surface.*

Keywords: *natural convective heat transfer, wavy surfaces, heat transfer enhancement,* $k-\varepsilon$ *turbulence model*

1. INTRODUCTION

Natural convection heat transfer occurs in many practical situations and remains an area of considerable basic and applied interest. In the present article, attention will be restricted to an external natural convective flow, in other words, a flow situation in which there are no constraining boundary surfaces near enough to the surface being considered to have any significant influence on the natural convective flow over this surface. Increasing the heat transfer rate in a given situation involving natural convective flows is often difficult to accomplish.

There are many ways to enhance natural convective heat transfer rate. The existent techniques work towards reducing the thermal resistance by increasing the convective heat transfer coefficient. Active techniques to achieve heat transfer enhancement demand the use of some external power, e.g. surface vibration and fluid vibration. On the other hand, passive techniques involve the use of surface or geometrical modifications, e.g. treated surfaces, rough surfaces and extended surfaces. In this context, using a wavy surface is one of the various methods of attempting to enhance natural convective heat transfer rates, being classified as a type of extended surface, more commonly known as finned surfaces. The extended surfaces are the most widely used and researched among the enhancement techniques, considered in most cases for cooling electrical and electronic devices; the study of these surfaces involve the analysis of the efficiency obtained with the specific shape, size and spacing between the waves (Bejan and Kraus, 2003). The presence of waves in the horizontal surface can really influence the physical behavior of the thermal plumes in the natural convection process, which is a key part on the heat transfer phenomenon. In that way, the altered shape of the thermal plumes can increase heat dissipation, enhancing the natural convection heat transfer rate (Kang and Jaluria, 1990).

The enhancement of the heat transfer rate produced by using a wavy surface arises from the increase in the surface area exposed to the fluid to which the heat is being transferred and, in some cases, to the changes in the near surface flow produced by the presence of the surface waves. The total enhancement of the heat transfer rate will depend on the shape and relative size of the surface waves. Many wavy shapes have been considered is past studies, but the most common shapes considered remain rectangular, triangular and sinusoidal waves. The enhancement of the heat transfer rate produced by using a wavy surface will also depend on the flow situation being considered, e.g. flow over a plane surface or flow over a cylinder, and on the thermal boundary conditions at the surface. The two surface boundary conditions most commonly considered are those in which there is uniform temperature over the surface and those in which there is uniform heat flux over the surface. Another factor that influences the natural convective heat transfer rate

from a surface is its orientation; the surface can be horizontal, vertical or inclined to the vertical and, when inclined, can be facing upward or downward (Oosthuizen, 2016).

While there have been some previous studies of natural convective heat transfer from a one-sided horizontal plate, these studies have mainly considered only the case where the plate is flat (non-wavy) and where the flow over the plate is laminar. Here, the conditions considered are such that laminar flow, transitional flow and turbulent flow can occur over the plate. Numerical studies of heat transfer from a horizontal surface having triangular waves and rectangular waves with constant height for conditions under which laminar, transitional, and turbulent flow exist are described in the works of Oosthuizen, (2016a) and Oosthuizen, (2016b), respectively. Other studies of natural convective heat transfer from horizontal wavy surfaces with constant height are described in the works of Prétot, *et al.* (2000), Prétot, *et al.* (2003), Siddiqa and Hossain (2013) and Siddiqa, *et al.*, (2015). A study of natural convective heat transfer from horizontal rectangular and triangular wavy surfaces with variable height is described in the work of Oliveira and Oosthuizen (2018). In all of these studies, the natural convective heat transfer rate was obtained from a one-side, two-dimensional horizontal plate having a uniform surface temperature.

The purpose of the present article is to develop a numerical study of natural convective heat transfer from a one-sided, two-dimensional horizontal plate having a uniform surface temperature. The surface shape is wavy, and attention has been given to the case where the surface waves have a trapezoidal shape with variable height. It is expected that waves with variable height can produce changes in the near surface flow and then promote and enhancement of the natural convective heat transfer rate. The temperature of the horizontal plate surface is higher than the temperature of the surrounding fluid. Results for three dimensionless surface wave profiles (linear, parabolic and exponential) will be obtained and used to determine whether the presence of the waves with variable height can produce an enhancement in the natural convective heat transfer rate compared to that from a plane (non-wavy) horizontal surface.

2. PHYSICAL SITUATION

The physical situation considered in this study is shown in Fig. 1:

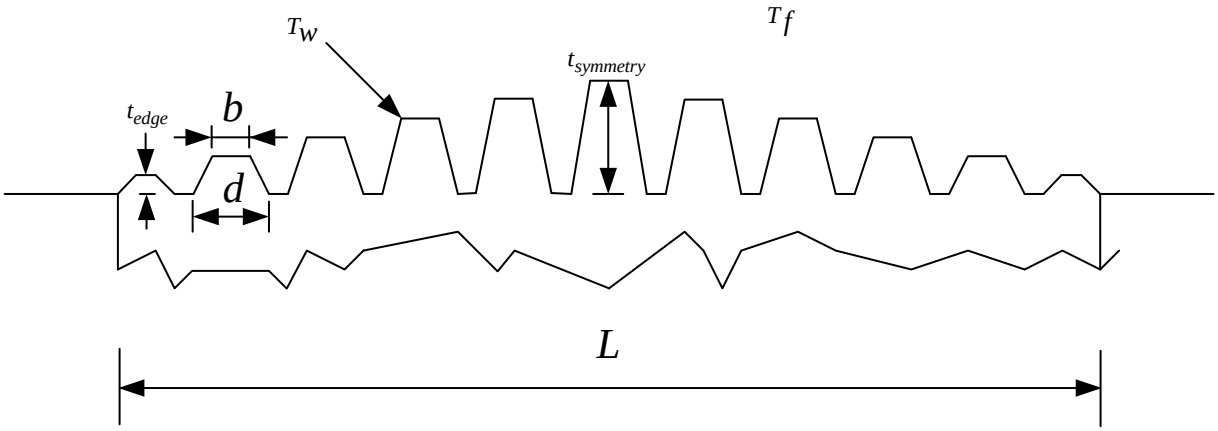

Figure 1. Horizontal surface with trapezoidal waves with variable height.

The situation here being considered consists of a two-dimensional horizontal plate having a uniform surface temperature T_w. The surface shape is wavy, and attention has been given to the case where the surface waves have a trapezoidal shape with variable height $t(x)$, larger base with width d and minor base with width b. The waves are equally spaced. The surface is in contact with a surrounding fluid at constant temperature T_f. For a heated surface, $T_w > T_f$, and the heated surface will exchange energy with the surrounding fluid by natural convection. The horizontal plate has unit width L and unit depth w. The purpose of this study is to calculate the mean heat transfer rate by natural convection between the heated surface and the surrounding fluid. Because the flow is assumed symmetrical about the centerline, only half of the horizontal plate width has been considered. The mean heat transfer rate q has been expressed in terms of mean Nusselt number based on the difference between the horizontal plate and surrounding fluid temperatures and on the projected area of the horizontal plate, that is:

$$\overline{\mathrm{Nu}}_{L_c} = \frac{qL_c}{kA_{projected}(T_w - T_f)} \tag{1}$$

Eq. (1) is a combination between the Newton law of cooling based on a projected area of the horizontal surface, i.e., *wL*, and the definition of the mean Nusselt number based on a characteristic width. In this work it was assumed that the characteristic width L_c is the width *L* of the horizontal surface.

The reason why the projected area of the horizontal surface is used instead of its wetted area is the fact that, if the true surface area was considered, the comparison between the heat transfer rate of the horizontal surfaces with trapezoidal waves and the non-wavy flat surface would not be reasonable, because the trapezoidal surfaces would have an advantage due to the their greater area. Using the projected area gives the possibility of analyzing how the trapezoidal waves help increasing the mean Nusselt number by the different natural convection flow pattern, not considering the increase of the superficial area. Furthermore, as the characteristic dimension for the non-wavy flat surface is its length, it is interesting to maintain the same characteristic dimension through the other surfaces analyzed for the sake of normalization.

In the initial situation considered, the shortest wave height, in dimensionless form, located on the edge of the horizontal surface, is $H_{\text{edge}} = t_{\text{edge}} / L = 0.02,$ and the tallest height, in dimensionless form, located on the half of the horizontal surface (on symmetry line), is $H_{\text{symmetry}} = t_{\text{symmetry}} / L = 0.10$ (Oliveira and Oosthuizen, 2018). To study the effect of the wave variable height, four additional geometric situations were considered, increasing the height of the wave located at the edge of the horizontal surface and decreasing the height of the wave located on the half of the horizontal surface.

In the first additional situation, it was considered $H_{\text{edge}} = 0.04$ and $H_{\text{symmetry}} = 0.08.$ Next, it was considered $H_{\text{edge}} = H_{\text{symmetry}} = 0.06,$ a horizontal wave surface with constant height. In the third additional situation, it was considered $H_{\text{edge}} = 0.08$ and $H_{\text{symmetry}} = 0.04.$ Lastly, it was considered $H_{\text{edge}} = 0.10$ and $H_{\text{symmetry}} = 0.02.$ For each situation, the wave height profile was varied (Oliveira and Oosthuizen, 2018).

With the values of H_{edge}, H_{symmetry} and its respective positions, $X_{\text{edge}} = x_{\text{edge}} / L$ and $X_{\text{symmetry}} = x_{\text{symmetry}} / L,$ three different wave profiles were used to calculate the height of the three internal waves: a linear profile, a parabolic profile and an exponential profile. It is worth to mention that, as the positions of each wave were normalized by the length of the horizontal surface, they are in dimensionless form as well as the wave heights, meaning that the capital letters H and X refer to dimensionless parameters. For a linear profile, a general expression can be written in a dimensionless form as:

$$H(X) = AX + B \tag{2}$$

where *A* and *B* are dimensionless coefficients that can be determined from the knowledge of $H_{\text{edge}}(X_{\text{edge}})$ e $H_{\text{symmetry}}(X_{\text{symmetry}}),$ that is:

$$A = \frac{H_{\text{edge}} - H_{\text{symmetry}}}{X_{\text{edge}} - X_{\text{symmetry}}} \tag{3}$$

$$B = H_{\text{edge}} - \left(\frac{H_{\text{edge}} - H_{\text{symmetry}}}{X_{\text{edge}} - X_{\text{symmetry}}} \right) X_{\text{edge}} \tag{4}$$

Substituting Eqs. (3-4) into Eq. (2) and rearranging:

$$H(X) = H_{\text{edge}} + \left(\frac{H_{\text{edge}} - H_{\text{symmetry}}}{X_{\text{edge}} - X_{\text{symmetry}}} \right) (X - X_{\text{edge}}) \tag{5}$$

For a parabolic profile, a general expression for the wave profile can be written in a dimensionless form as:

$$H(X) = AX^2 + BX + C \tag{6}$$

where *A*, *B* and *C* are dimensionless coefficients that can be determined from the knowledge of $H_{\text{edge}}(X_{\text{edge}}),$ $H_{\text{symmetry}}(X_{\text{symmetry}})$ and $(dH/dX)_{X=X_{\min}} = 0,$ where $X_{\min} = X_{\text{edge}}$ if $H_{\text{edge}} < H_{\text{symmetry}}$ and $X_{\min} = X_{\text{symmetry}}$ if $H_{\text{edge}} > H_{\text{symmetry}},$ that is:

$$A = \frac{H_{\text{edge}} - H_{\text{symmetry}}}{X_{\text{edge}}^2 - X_{\text{symmetry}}^2 - 2X_{\min}(X_{\text{edge}} - X_{\text{symmetry}})} \tag{7}$$

$$B = -\frac{2X_{\min}(H_{\text{edge}} - H_{\text{symmetry}})}{X_{\text{edge}}^2 - X_{\text{symmetry}}^2 - 2X_{\min}(X_{\text{edge}} - X_{\text{symmetry}})} \tag{8}$$

$$C = H_{\text{edge}} + \left[\frac{H_{\text{edge}} - H_{\text{symmetry}}}{X_{\text{edge}}^2 - X_{\text{symmetry}}^2 - 2X_{\min}(X_{\text{edge}} - X_{\text{symmetry}})}\right](2X_{\min}X_{\text{edge}} - X_{\text{edge}}^2) \tag{9}$$

Substituting Eqs. (7-9) into Eq. (6) and rearranging:

$$H(X) = H_{\text{edge}} + \left[\frac{H_{\text{edge}} - H_{\text{symmetry}}}{X_{\text{edge}}^2 - X_{\text{symmetry}}^2 - 2X_{\min}(X_{\text{edge}} - X_{\text{symmetry}})}\right](X^2 - 2X_{\min}X + 2X_{\min}X_{\text{edge}} - X_{\text{edge}}^2) \tag{10}$$

For an exponential profile, a general expression for the wave profile can be written in a dimensionless form as:

$$H(X) = AX^B \tag{11}$$

where A and B are dimensionless coefficients that can be determined from the knowledge of $H_{\text{edge}}(X_{\text{edge}})$ and $H_{\text{symmetry}}(X_{\text{symmetry}})$, that is:

$$A = \frac{H_{\text{edge}}}{\left(\frac{H_{\text{edge}}}{H_{\text{symmetry}}}\right)^{\left(\frac{X_{\text{edge}}}{X_{\text{edge}} - X_{\text{symmetry}}}\right)}} \tag{12}$$

$$B = \left(\frac{H_{\text{edge}}}{H_{\text{symmetry}}}\right)^{\left(\frac{1}{X_{\text{edge}} - X_{\text{symmetry}}}\right)} \tag{13}$$

Substituting Eqs. (12-13) into Eq. (11) and rearranging:

$$H(X) = H_{\text{edge}}\left(\frac{H_{\text{edge}}}{H_{\text{symmetry}}}\right)^{\left(\frac{X - X_{\text{edge}}}{X_{\text{edge}} - X_{\text{symmetry}}}\right)} \tag{14}$$

Equations (5), (10) and (14) can be used to determine the height of the internal trapezoidal waves. For each trapezoidal wave, the point of height considered is located in the center of each horizontal segment of the corresponding height. According to the dimensions considered, the wave profile equations used for the trapezoidal waves can be seen in Tab. 1. To verify the profile that is most suitable for the increase of the heat transfer rate by natural convection, it is convenient to name the wave height profiles as follows:

- For $H_{\text{edge}} = 0.00$ and $H_{\text{symmetry}} = 0.00$: PROFILE 0 (non-wavy flat plate)
- For $H_{\text{edge}} = 0.02$ and $H_{\text{symmetry}} = 0.10$: PROFILE 1
- For $H_{\text{edge}} = 0.04$ and $H_{\text{symmetry}} = 0.08$: PROFILE 2
- For $H_{\text{edge}} = 0.06$ and $H_{\text{symmetry}} = 0.06$: PROFILE 3 (constant wave height)
- For $H_{\text{edge}} = 0.08$ and $H_{\text{symmetry}} = 0.04$: PROFILE 4
- For $H_{\text{edge}} = 0.10$ and $H_{\text{symmetry}} = 0.02$: PROFILE 5

It should be noted that the expressions provided in Tab. 1 were developed for the specific case of ten trapezoidal waves considering the whole plate.

Table 1. Wave profile equations for trapezoidal waves.

PROFILE NUMBER	GEOMETRY	PROFILE EQUATIONS
PROFILE 1	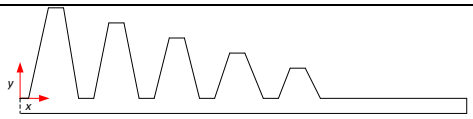	$H(X) = -0.1933X + 0.1100$ $H(X) = 0.4672X^2 - 0.4350X + 0.1212$ $H(X) = 0.1223(0.0205^X)$
PROFILE 2	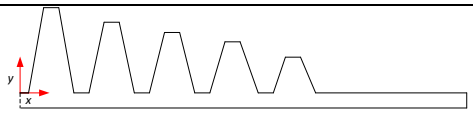	$H(X) = -0.0967X + 0.0850$ $H(X) = 0.2336X^2 - 0.2175X + 0.0906$ $H(X) = 0.0872(0.1873^X)$
PROFILE 3	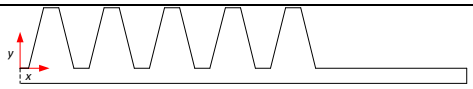	$H(X) = 0.06$
PROFILE 4	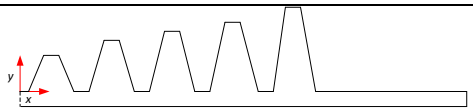	$H(X) = 0.0967X + 0.0350$ $H(X) = 0.2336X^2 - 0.0242X + 0.0406$ $H(X) = 0.0367(5.3394^X)$
PROFILE 5	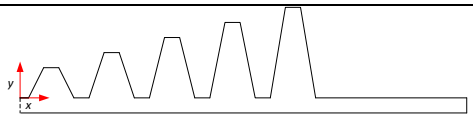	$H(X) = 0.1933X + 0.0100$ $H(X) = 0.4672X^2 - 0.0483X + 0.0212$ $H(X) = 0.0164(48.8852^X)$

3. SOLUTION PROCEDURE

In obtaining the numerical results, the mean flow has been assumed to be steady and the Boussinesq approximation has been used, i.e., fluid properties have been assumed to be constant except for the density change with temperature that gives rise to the buoyancy forces, the density change being assumed to be proportional to the temperature change. Radiation heat transfer effects have been neglected. Allowance has been made for the possibility that turbulent flow can occur in the system. In order to deal with this, the basic $k-\varepsilon$ turbulence model with standard wall functions and full account being taken of buoyancy force effects has been used. The governing equations subject to the boundary conditions have been solved numerically using the commercial CFD solver ANSYS FLUENT©. In all cases, extensive grid independence and convergence-criteria independence testing was undertaken. The numerical approach used here in order to determine when turbulence develops involves solving the Reynolds averaged governing equations together with a turbulence model, in which the effects of buoyancy forces are taken into account, for all conditions considered, then monitoring the results obtained with increasing Rayleigh numbers to determine when significant turbulence effects develop. This approach has been used quite extensively in the study of forced convective flows, e. g., see Schmidt and Patankar (1991) and Zheng *et al.* (1998). The Nusselt number in any situation will depend on:

1. The Rayleigh number, Ra_L, based on the reference length scale L of the heated surface and the difference between the temperature of the heated isothermal surface, T_w, and the temperature of the undisturbed fluid well away from the system, T_f, i.e.:

$$\mathrm{Ra}_L = \frac{g\beta(T_w - T_f)L^3}{\nu\alpha} \tag{15}$$

2. The dimensionless width of the larger base, $D = d/L$.
3. The dimensionless width of the minor base, $B = b/L$.
4. The dimensionless height of the surface waves, $H = t/L$ and
5. The Prandtl number, Pr.

In Eq. (15), Ra_L is the Rayleigh number based on L, g is the gravitational acceleration, β is the bulk coefficient of thermal expansion, L is the width of the heated surface, ν is the kinematic viscosity of the fluid and α is the thermal diffusivity of the fluid. Results have only been obtained for a Prandtl number of 0.74, i.e., effectively the value for air. All the results obtained for the wave surfaces were compared with results obtained for the same surface without waves, in terms of the a mean Nusselt number.

Before obtaining numerical results, a mesh independence study was carried out using the highest Rayleigh number value, i.e., 10^{12}, for a case with constant wave height (profile 3). Results of the mesh independence test can be seen in Tab. 2:

Table 2. Mesh independence test.

Number of elements	$\overline{\mathrm{Nu}}_L$
200000	1910
300000	2135
400000	2190
500000	2200
600000	2210

According to Tab. 2, for approximately 500000 elements, the mean Nusselt number remained approximately constant. This number of elements was then used in all numerical simulations. In all simulations, the mean Nusselt number integrated over the surface was monitored to ensure convergence and to verify that the simulation reached the steady state. The complete computational domain is 4 m length and 2 m high. By symmetry, half of the computational domain was simulated. The configuration of the ANSYS FLUENT© solver was based on the work of Oliveira and Oosthuizen (2018), Oosthuizen (2016), Oosthuizen (2016a) and Oosthuizen (2016b), having already been extensively tested and validated with results of numerical and experimental works by these authors. The convergence criteria used for all variables in numerical simulations was 10^{-5}.

4. RESULTS AND DISCUSSION

The horizontal surfaces, wavy and non-wavy, are thin with unit width L and unit depth w maintained at a uniform surface temperature $T_w = 310$ K. The surrounding fluid is air at a temperature $T_f = 290$ K at atmospheric pressure. Numerical simulations were performed for Rayleigh numbers varying between 10^6 to 10^{12}. Numerical results for natural convective heat transfer rate from the surface with trapezoidal waves were obtained by fixing $D = 2B$ and using fourteen different profiles for $H(X)$, that is, four linear, four parabolic, four exponential, one constant and one flat. The width of the adiabatic part is one meter on both sides of the horizontal surface.

The behavior of the mean Nusselt number as a function of the Rayleigh number for different trapezoidal wave height profiles can be seen in Figs. 2, 4 and 6. As it was mentioned before, Profile 0 represents the non-wavy flat plate and Profile 3 represents the case with constant wave height. Applying the least squares method to the data obtained, Figs. 2, 4 and 6 were converted to Figs 3, 5 and 7, respectively. As it can be seen in the Figs. 2 to 7, the mean Nusselt number increases as the Rayleigh number intensifies, presenting a crescent behavior, for all profiles. A better graphical comparison can be done analyzing the content of Figs. 8 to 13, in which the mean Nusselt number is represented as a function of a given profile for different Rayleigh numbers.

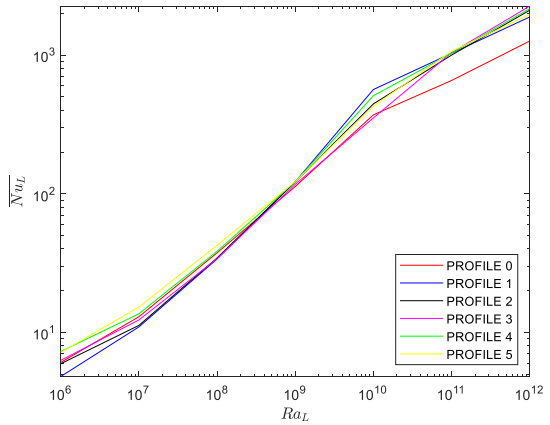

Figure 2. Variations of mean Nusselt number with Rayleigh number for various trapezoidal wave linear profiles.

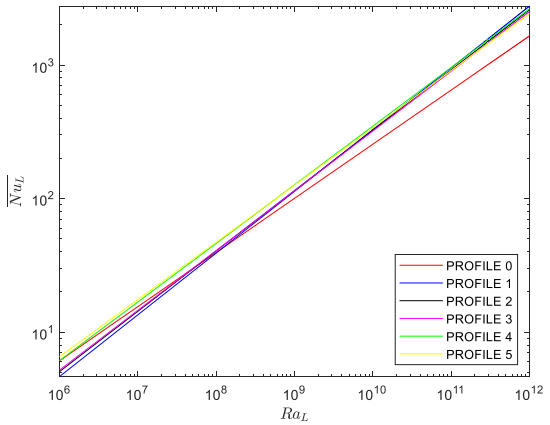

Figure 3. Variations of mean Nusselt number with Rayleigh number for various trapezoidal wave linear profiles (least squares method applied).

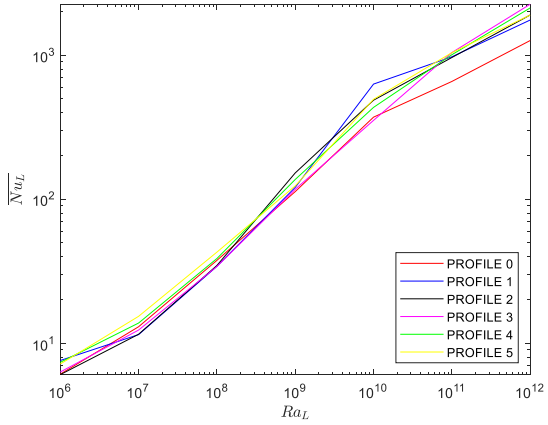

Figure 4. Variations of mean Nusselt number with Rayleigh number for various trapezoidal wave parabolic profiles.

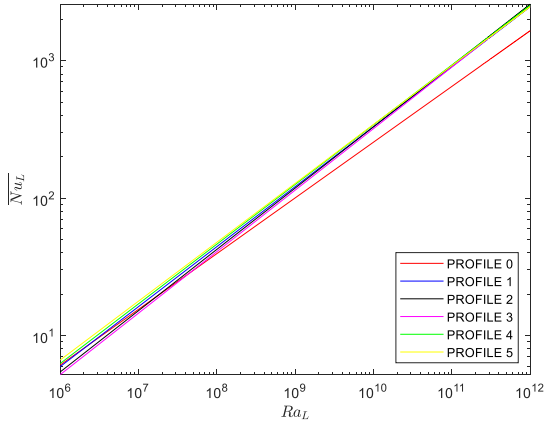

Figure 5. Variations of mean Nusselt number with Rayleigh number for various trapezoidal wave parabolic profiles (least squares method applied).

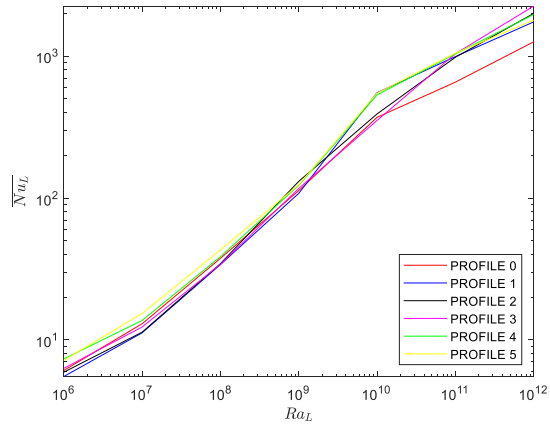

Figure 6. Variations of mean Nusselt number with Rayleigh number for various trapezoidal wave exponential profiles.

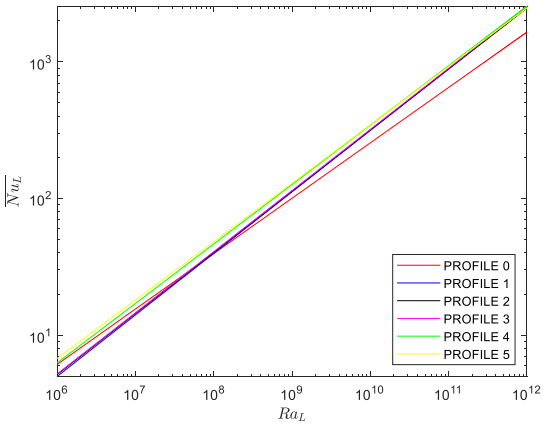

Figure 7. Variations of mean Nusselt number with Rayleigh number for various trapezoidal wave exponential profiles (least squares method applied).

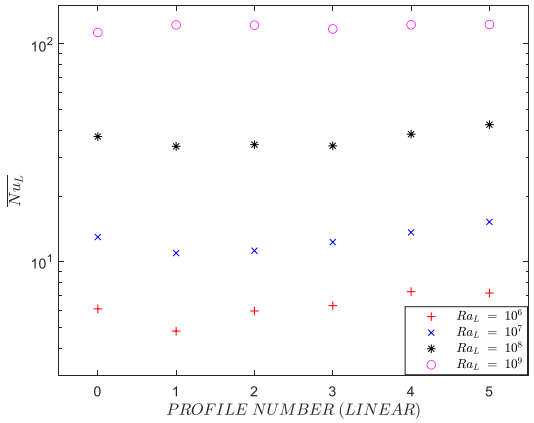

Figure 8. Variations of mean Nusselt number with trapezoidal wave linear profiles for Rayleigh numbers of 10^6, 10^7, 10^8 and 10^9.

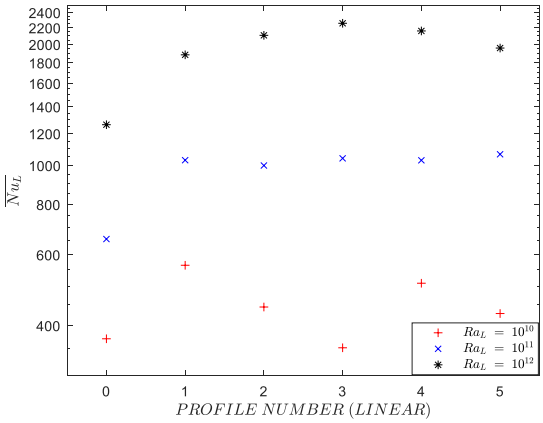

Figure 9. Variations of mean Nusselt number with trapezoidal wave linear profiles for Rayleigh numbers of 10^{10}, 10^{11} and 10^{12}.

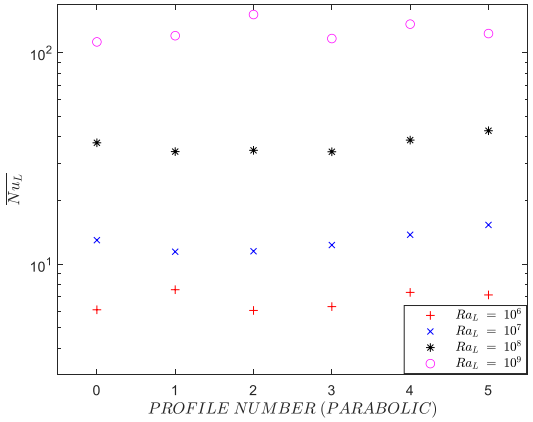

Figure 10. Variations of mean Nusselt number with trapezoidal wave parabolic profiles for Rayleigh numbers of 10^6, 10^7, 10^8 and 10^9.

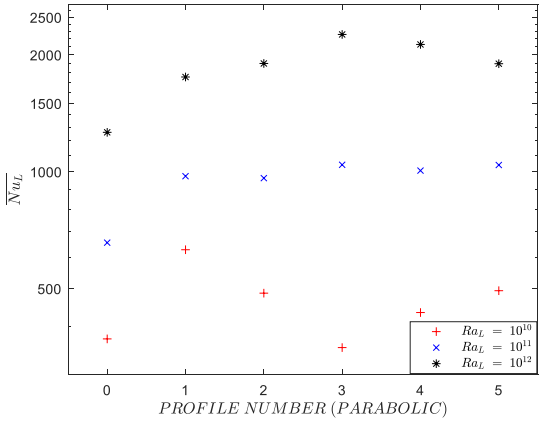

Figure 11. Variations of mean Nusselt number with trapezoidal wave parabolic profiles for Rayleigh numbers of 10^{10}, 10^{11} and 10^{12}.

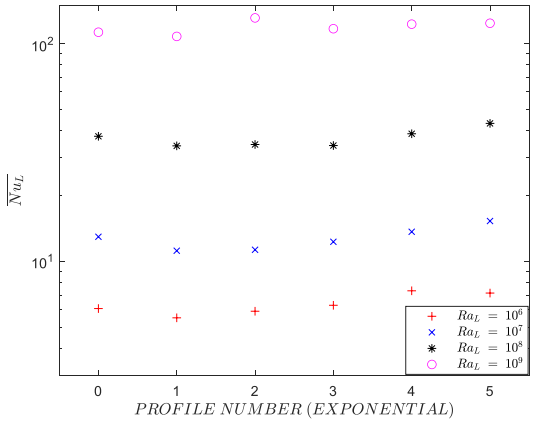

Figure 12. Variations of mean Nusselt number with trapezoidal wave exponential profiles for Rayleigh numbers of 10^6, 10^7, 10^8 and 10^9.

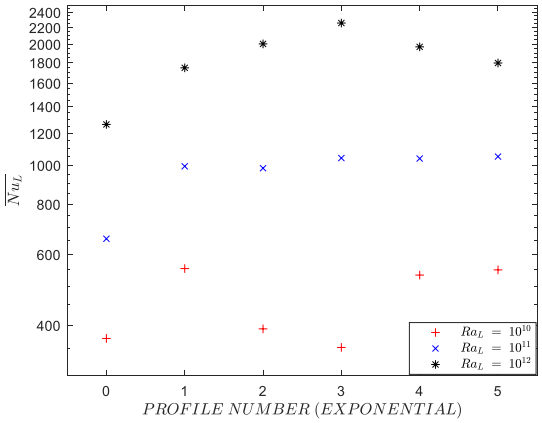

Figure 13. Variations of mean Nusselt number with trapezoidal wave exponential profiles for Rayleigh numbers of 10^{10}, 10^{11} and 10^{12}.

With the application of the least square method, it was possible to provide correlations between the mean Nusselt number and the Rayleigh number to all fourteen profiles. Correlations were written in form of $\overline{\mathrm{Nu}}_L = C\mathrm{Ra}_L^n$, where C and n are constants provided by the method. The list of all correlations obtained can be seen in Tab. 3.

For a more accurate comparison between the profiles, the percentage increases in the mean Nusselt number for all profiles in relation to the non-wavy flat surface (Profile 0), for Rayleigh numbers between 10^6 and 10^{12}, were shown in Tab. 4.

As it was mentioned before, it was considered the projected area of the surface rather than the wetted area to calculate the mean Nusselt number, giving the possibility to analyze the true contribution of the trapezoidal waves in the natural convection heat transfer rate of the surface instead of the sheer contribution of the increased area. It is possible to see in Tab. 4 that the mean Nusselt number, for various profiles and Rayleigh numbers, was lower than the presented by the non-wavy flat surface, represented by a negative value in the percentage increase. The reason for that is, as the areas between all surfaces are normalized, the natural convection flow is less effective in some trapezoidal profiles than in the non-wavy flat surface, possibly because of a flow difficulty due to the presence of the waves.

Table 3. Correlation between the Nusselt number and the Rayleigh number for the different profiles.

PROFILE NUMBER	TYPE OF FUNCTION	CORRELATION
PROFILE 0	Linear	$\overline{\mathrm{Nu}}_L = 0.02251\mathrm{Ra}_L^{0.4055}$
PROFILE 1	Linear	$\overline{\mathrm{Nu}}_L = 0.007813\mathrm{Ra}_L^{0.4624}$
	Parabolic	$\overline{\mathrm{Nu}}_L = 0.01432\mathrm{Ra}_L^{0.4364}$
	Exponential	$\overline{\mathrm{Nu}}_L = 0.009887\mathrm{Ra}_L^{0.4503}$
PROFILE 2	Linear	$\overline{\mathrm{Nu}}_L = 0.009821\mathrm{Ra}_L^{0.4520}$
	Parabolic	$\overline{\mathrm{Nu}}_L = 0.01148\mathrm{Ra}_L^{0.4459}$
	Exponential	$\overline{\mathrm{Nu}}_L = 0.01065\mathrm{Ra}_L^{0.4473}$
PROFILE 3	Linear	$\overline{\mathrm{Nu}}_L = 0.01072\mathrm{Ra}_L^{0.4476}$
PROFILE 4	Linear	$\overline{\mathrm{Nu}}_L = 0.01422\mathrm{Ra}_L^{0.4390}$
	Parabolic	$\overline{\mathrm{Nu}}_L = 0.01551\mathrm{Ra}_L^{0.4343}$
	Exponential	$\overline{\mathrm{Nu}}_L = 0.01531\mathrm{Ra}_L^{0.4352}$
PROFILE 5	Linear	$\overline{\mathrm{Nu}}_L = 0.01757\mathrm{Ra}_L^{0.4285}$
	Parabolic	$\overline{\mathrm{Nu}}_L = 0.01785\mathrm{Ra}_L^{0.4284}$
	Exponential	$\overline{\mathrm{Nu}}_L = 0.01832\mathrm{Ra}_L^{0.4277}$

Tab 4. Percentage increase in the Nusselt number of the different profiles for Rayleigh numbers between 10^6 and 10^{12} in comparison to Profile 0 (non-wavy flat plate).

RAYLEIGH NUMBER		10^6	10^7	10^8	10^9	10^{10}	10^{11}	10^{12}
PROFILE 1	Linear	-20.90%	-15.54%	-9.78%	8.27%	52.32%	57.05%	49.18%
	Parabolic	24.46%	-11.80%	-9.15%	7.01%	69.71%	48.35%	38.84%
	Exponential	-9.33%	-13.72%	-9.62%	-4.34%	49.2%	51.41%	38.26%
PROFILE 2	Linear	-2.19%	-13.39%	-8.20%	7.99%	19.94%	52.34%	66.78%
	Parabolic	-0.73%	-11.34%	-7.89%	34.76%	31.17%	46.63%	50.44%
	Exponential	-2.79%	-12.84%	-8.32%	16.31%	5.64%	49.77%	58.59%
PROFILE 3	Linear	3.51%	-5.16%	-9.31%	3.75%	-5.02%	58.72%	78.70%
PROFILE 4	Linear	19.96%	5.08%	2.55%	8.38%	37.44%	56.95%	71.03%
	Parabolic	20.86%	6.10%	2.96%	21.39%	16.93%	53.34%	68.41%
	Exponential	20.63%	5.42%	2.70%	8.88%	43.75%	58.28%	55.92%
PROFILE 5	Linear	18.20%	17.35%	13.36%	8.75%	15.55%	62.45%	55.08%
	Parabolic	17.56%	18.11%	14.04%	9.54%	33.10%	58.51%	50.23%
	Exponential	17.79%	18.08%	14.60%	9.96%	48.09%	60.09%	42.15%

For lower values of Rayleigh number, between 10^6 and 10^8, it can be seen in Tab. 4 that the percentage increase of mean Nusselt number is negative for profiles 1, 2 and 3, with the exception of profile 1 with parabolic function and profile 3 for a Rayleigh number of 10^6, which shows that these profiles are not quite suited for this range of Rayleigh numbers, although profile 1 with parabolic function has the greatest percentage increase among all other surfaces for a Rayleigh number of 10^6. On the other hand, profile 4 has high percentage increases for a Rayleigh number of 10^6 for all types of functions. For a Rayleigh number of 10^7 and 10^8, profile 5 presents the greatest percentage increases, with the highest value shown by the parabolic function for a Rayleigh number of 10^7 and by the exponential function for a Rayleigh number of 10^8.

For a Rayleigh number of 10^9, each surface presented a different behavior. It is possible to notice in Tab. 4 that the lowest value is presented by profile 1 with the exponential function, being the only one to show a negative value. The

greatest value is presented by profile 2 with the parabolic function, a considerable amount ahead of the second place, profile 4 with parabolic function.

For a Rayleigh number of 10^{10}, high values of percentage increases start to appear, greater than 50%, which are presented by profile 1 with functions both linear and parabolic, but the parabolic function is 15% percent ahead of the linear function. Being in the turbulent regime appears to help increasing the mean Nusselt number, which means that the occurrence of turbulence in the trapezoidal waves creates a condition of natural convective flow that favor the heat transfer rate. The only exception was profile 3, that presented negative value for the percentage increase. For the Rayleigh number of 10^{11}, more turbulence occurs, providing even greater percentage increases of the mean Nusselt number, as in this case every surface has at least 45% of increase, which means that there is no negative value either. profile 5 with linear function has the best percentage increase value for this Rayleigh number.

Lastly, for the Rayleigh number of 10^{12}, all of the surfaces presented a positive value of percentage increase, but not every value was an improvement in comparison to the results from the Rayleigh number of 10^{11}. The greatest value for the Rayleigh number of 10^{12} was presented by profile 3, being the maximum value of percentage increase among all Rayleigh number and all surfaces.

The results of Tab. 4 show that there is a most efficient surface for every Rayleigh number tested; there was no Rayleigh number in which every percentage increase was negative, so there is always a recommended surface to use instead of profile 0. Although it is possible to recommend specific surfaces for each case, it is interesting to notice that the profile that has the highest mean percentage increase is profile 5 with the exponential function, presenting 30.11% of increase in the mean Nusselt number in comparison to profile 0. Profiles 4 and 5, for all types of function, have at least 27% of mean percentage increase, while all other surfaces have between 15% and 20% of mean percentage increase. It shows that the crescent layout (presented by profiles 4 and 5) is more efficient than the descendent layout (presented by profiles 1 and 2). Finally, profiles 4 and 5, for all types of function, are the only to not present a negative value of percentage increase.

About the use of variable height profiles, the results show that it is very effective. There was only one Rayleigh number where the constant height profile was more effective, 10^{12}, which shows that the variation of the height of the trapezoidal waves helped the natural convection heat transfer hate in the majority of the cases. The numerical analysis of this work is an initial study. For the next steps of this research, it is necessary the development of an experimental study to validate the results obtained here.

5. CONCLUSIONS

The numerical analysis of the natural convective heat transfer from horizontal surfaces containing trapezoidal waves with variable height presented great results. As it was discussed, for Rayleigh numbers between 10^6 and 10^{11}, the variable height profiles presented significant percentage increase in the mean Nusselt number of the surface in comparison to the non-wavy flat surface, surpassing the percentage increase presented by the constant height wave profile. However, for a Rayleigh number of 10^{12}, the variable height trapezoidal wave profiles presented lower percentage increase of the mean Nusselt number in comparison to the constant height trapezoidal wave profile.

For specific applications, it is possible to recommend a profile and a function based on the Rayleigh number for the situation: profile 1 with parabolic function for 10^6, profile 5 with parabolic function for 10^7, profile 5 with exponential function for 10^8, profile 2 with parabolic function for 10^9, profile 1 with parabolic function for 10^{10}, profile 5 with linear function for 10^{11} and profile 3 for 10^{12}. For an overall great performance, it is recommended to use profile 5 with exponential function, being the surface with the highest mean percentage increase of the mean Nusselt number in comparison to the non-wavy flat surface.

Further conclusions could be provided with more numerical studies. It would be interesting to analyze the performance obtained with different ratios between the minor and the larger base of the waves and with different numbers of trapezoidal waves.

6. ACKNOWLEDGEMENTS

This work was supported by FAPESP (Fundação de Amparo à Pesquisa do Estado de São Paulo) under grant 2019/16137-1.

7. REFERENCES

Bejan, A. and Allan, D. K., 2003. “Heat transfer handbook”. John Wiley & Sons, Vol. 1, p. 1030-1033, p. 1059-1061.

Kang, B. H. and Jaluria, Y., 1990. "Natural convection heat transfer characteristics of a protruding thermal source located on horizontal and vertical surfaces." International journal of heat and mass transfer, Vol. 33, p. 1347-1357.

Oliveira, S.D.R. and Oosthuizen, P.P, 2018. “A numerical study of the natural convective heat transfer from the surface of a thin horizontal plate having a wavy surface with variable height”. In *17th Brazilian Congress of Thermal Sciences and Engineering* – ENCIT 2018, Águas de Lindóia, Brazil.

Oosthuizen, P.H., 2016. "External natural convective heat transfer from bodies having a wavy surface for conditions under which laminar, transitional, and turbulent flow can exist". *Advances in Heat Transfer*, Vol. 48, p. 261-317.

Oosthuizen, P.H., 2016a. "A numerical study of natural convective heat transfer from a horizontal isothermal surface with rectangular surface roughness elements". In Proceedings of the First Pacific Rim Thermal Engineering Conference - PRTEC 2016, Hawaii's Big Island, USA.

Oosthuizen, P.H., 2016b. "A numerical study of the effect of triangular waves on natural convective heat transfer from an upward facing heated horizontal isothermal surface". In ASME 2016 International Mechanical Engineering Congress and Exposition, Phoenix, USA.

Prétot, S., Zeghmati, B. and Caminat, Ph., 2000. "Influence of surface roughness on natural convection above a horizontal plate". Advances in Engineering Software, Vol. 30, p. 793-801.

Prétot, S., Miriel, J., Baily, Y. and Zeghmati, B., 2003. "Visualization and simulation of the natural convection flow above horizontal wavy plates". Numerical Heat Transfer, Part A: Applications, Vol. 43, p. 307-325.

Siddiqa, S. and Hossain, M.A., 2013. "Natural convection flow over wavy horizontal surface". Advances in Mechanical Engineering, Vol. 5, p. 1-7.

Schmidt, R. C. and Patankar, S. V., 1991. "Simulating boundary layer transition with low-Reynolds-Number k-ε turbulence models: Part 1- an evaluation of prediction characteristics". *ASME Journal of Turbomachinery*, Vol. 113, p. 10-17.

Siddiqa, S., Hossain, M.A. and Gorla, R.S.R., 2015. "Natural convection flow of viscous fluid over triangular wavy horizontal surface". *Computers & Fluids*, Vol. 5, p. 130-134.

Zheng, X., Liu, C., Liu, F. and C.-I. Yang., 1998. "Turbulent transition simulation using the k-ω model". *International Journal for Numerical Methods in Engineering*, Vol. 42, p. 907-926.

8. RESPONSIBILITY NOTICE

The authors are the only responsible for the printed material included in this paper.